Table II. Spectral Characteristics for Complexes 1–3

compd	IR,[a] cm^{-1}	^{1}H NMR[b,c]		^{13}C{^{1}H} NMR[b,c]		^{31}P NMR[b,d]
		δ, ppm	J_{P-H}, Hz (mult)	δ, ppm	J_{P-C}, Hz (mult)	δ, ppm (mult)
1	2020 (s)	3.57 (OCH$_3$)	60 (t)	211.9 (CO)^e	18 (t)	188.0 (t)
	1975 (s)	−11.2 (Fe–H)				
2	2020 (s)	1.25 (CH$_3$)	60 (t)	212.5 (CO)^f	18 (t)	182.2 (t)
	1970 (s)	3.93 (OCH$_2$)				
		−11.0 (Fe–H)				
3	2040 (s)	7.2 (OC$_6$H$_5$)	62 (t)	209.0 (CO)^g	16 (t)	175.1 (t)
	1990 (s)	−11.3 (Fe–H)				

^{a} Pentane solution for **1** and **2**; KBr pellet for **3**. ^{b} CDCl$_3$ solution. ^{c} Relative to TMS. ^{d} Relative to H$_3$PO$_4$. ^{e} Other signal at 51.5 ppm (s) (OCH$_3$). ^{f} Other signals at 60.3 ppm (s) (OCH$_2$) and 15.8 ppm (t) (CH$_3$). ^{g} Other signals for aromatic carbons (s) at 151.5 ppm (C–O), 129.4 ppm (C ortho), 124.4 ppm (C para), and 121.6 ppm (C meta).

Discussion

To the best of our knowledge, only one synthesis of **1** has been previously reported, which gives a moderate yield and involves a much more tedious procedure (eqs 3 and 4).[6]

$$Fe(CO)_3[P(OMe)_3]_2 \xrightarrow[\text{Et}_2O, -80\,°C]{h\nu,\ N_2}$$
$$(CO)_2[P(OMe)_3]_2Fe-N_2-Fe(CO)_2[P(OMe)_3]_2 \quad (3)$$
$$(19\%)$$

$$(CO)_2[P(OMe)_3]_2Fe-N_2-Fe(CO)_2[P(OMe)_3]_2 \xrightarrow[\text{25 °C, 12 h}]{\text{Et}_2O,\ H_2\ (1\ atm)}$$
$$H_2Fe(CO)_2[P(OMe)_3]_2 \quad (4)$$
$$\mathbf{1}\ (45\%)$$
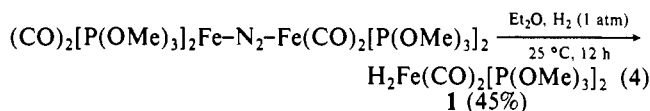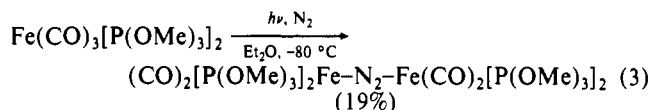
Two other complexes of the series H$_2$Fe(CO)$_2$[P(OR)$_3$]$_2$ are known [P(OR)$_3$ = P(OPh)$_3$, P(OCH$_2$)$_3$CC$_2$H$_5$].[8] They have been prepared in good yield (e.g. for P(OPh)$_3$, see eq 5), but their synthesis involves the cumbersome preparation of the unstable H$_2$Fe(CO)$_4$ complex just before use.[8]

$$H_2Fe(CO)_4 + 2P(OPh)_3 \xrightarrow[\text{room temp., 30 min}]{\text{ligroin}}$$
$$H_2Fe(CO)_2[P(OPh)_3]_2 \quad (5)$$
$$\mathbf{3}\ (89\%)$$
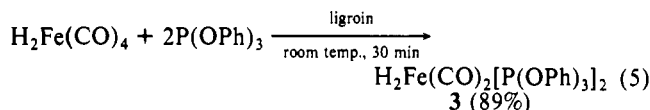
Thus, the reaction of the readily available K[HFe(CO)$_4$] with phosphites in a protic medium appears to be the best method for the high-yield, expedient synthesis of H$_2$Fe(CO)$_2$[P(OR)$_3$]$_2$ complexes.

Experimental Section

Materials and Methods. Iron pentacarbonyl (Aldrich) and potassium hydroxide (Prolabo, 86%) were used as received. Phosphites (Fluka) were purified by distillation, and all solvents were degassed under argon just before use. All manipulations were conducted by using Schlenk tube techniques. ^{1}H, ^{13}C, and ^{31}P NMR spectra were recorded on a Bruker WH 90 spectrometer. The IR spectra were recorded on a Perkin-Elmer 597 spectrometer. GC analyses were performed on an Intersmat IGC 16 gas chromatograph (catharometer) fitted with a 2 m × $^1/_8$ in. column containing 5-Å molecular sieves (40–60 mesh) with helium as carrier gas.

Synthesis of Complexes 1–3. Iron pentacarbonyl (1.5 mL, 11 mmol) was added to a solution of potassium hydroxide (1.47 g, 22 mmol) in 80 mL of a H$_2$O/THF (50/30 mL) mixture previously degassed under argon for 0.5 h. After the mixture was stirred for 0.5 h at 25 °C, the IR spectra (0.05 mm CaF$_2$ windows) of the pale pink reaction medium exhibited the absorption bands expected for K[HFe(CO)$_4$] (2000 vw, 1920 sh, 1900 s cm^{-1}).[9] The phosphite (22 mmol) was then added with a syringe through a serum cap, and the Schlenk tube was immediately connected to a gas buret. A gas, which was later identified as pure carbon monoxide (GC analysis) was evolved (520 mL, 22 mmol) within 1 h (R = Me, Et) or 24 h (R = Ph) after ligand addition. The reaction was complete when gas evolution had ceased.

The organic solvent was then evaporated slowly under reduced pressure (caution, the reaction products **1–3** easily sublime!) up to the appearance of a milk-like precipitate (R = Me, Et) or precipitation of white crystals (R = Ph). For R = Me or Et, the reaction products were extracted with pentane (6 × 30 mL) under argon. After careful concentration to 50 mL, the solution was cooled to −78 °C for 3 h, during which white crystals precipitated. The light green pentane solution was

removed by syringe, and the products were dried at −20 °C under reduced pressure. For R = Ph, water was removed by syringe, and the white crystals were dissolved in 40 mL of THF. The solution was transferred by syringe to another Schlenk tube and concentrated to 20 mL. Addition of 40 mL of pentane and cooling in the refrigerator overnight precipitated again white crystals of **3**, which were separated, washed with cold pentane, and dried as above. **1** and **2** were obtained as colorless oils, and **3** was obtained as white crystals (see Table I).

Contribution from the Department of Chemistry,
University of Florence, Florence, Italy,
and Department of Chemistry,
University of Modena, Modena, Italy

Ferromagnetic Coupling of Gadolinium(III) Ions and Nitronyl Nitroxide Radicals in an Essentially Isotropic Way

Cristiano Benelli, Andrea Caneschi, Antonio Costantino Fabretti, Dante Gatteschi,* and Luca Pardi

In the last few years, we reported a few compounds in which gadolinium(III) is magnetically coupled with either copper(II)[1,2] ions or nitronyl nitroxide radicals,[3,4] and in all cases we found that the sign of the coupling constant, defined by the isotropic Hamiltonian $H = JS_1\cdot S_2$, is negative; i.e., the spins in the pairs tend to align parallel to each other. The origin of the ferromagnetic coupling has been attributed to the fact that the magnetic orbital of either the copper(II) ion or the radical has nonzero overlap with the gadolinium(III) 7s orbital:[5,6] the fraction of unpaired electron that is transferred in the empty orbital polarizes the 4f electron spins, forcing them to be parallel to the copper or radical unpaired spins according to Hund's rule.

Since the extent of the observed coupling is on the order of 0.1–1 cm^{-1}, and since in the compounds reported so far the gadolinium(III) ion interacts with more than one paramagnetic ligand, it was not possible to evaluate accurately the possible role of the dipolar interactions between the spins in determining the observed magnetic properties.[7] We have now synthesized Gd(hfac)$_3$-(NITiPr)(H$_2$O) (hfac = hexafluoroacetylacetonate, NITiPr = 2-isopropyl-4,4,5,5-tetramethyl-4,5-dihydro-1*H*-imidazoyl-1-oxyl 3-oxide) in which one metal ion interacts with one radical, allowing for a more accurate analysis of the nature of the magnetic interaction between gadolinium and nitronyl nitroxides. We report here the structure of the isomorphous Eu(hfac)$_3$(NITiPr)(H$_2$O), which yielded better crystals, and analyze the magnetic properties of Gd(hfac)$_3$(NITiPr)(H$_2$O).

Experimental Section

Synthesis. The NITiPr radical was prepared as previously described[8,9] and identified by melting point and EPR spectrum.

(9) Darensbourg, M. Y.; Darensbourg, D. J.; Barros, L. C. *Inorg. Chem.* **1978**, *17*, 297.

*To whom correspondence should be addressed at the University of Florence.

formula	$C_{25}H_{24}EuF_{18}N_2O_9$	fw	990.41
a, Å	16.148 (4)	space group	$P2_1/a$ (No. 14)
b, Å	14.559 (5)	T, °C	22
c, Å	17.629 (4)	λ, Å	0.71069
β, deg	115.65 (2)	ρ_{calc}, g cm⁻³	1.76
V, Å³	3736.25	μ, cm⁻¹	16.9
Z	4	R	0.0774
		R_w	0.0781

M(hfac)₃·H₂O (M = Eu, Gd) were prepared according to the literature method[10] and satisfactorily analized for C, H, and N.

One millimole of the rare-earth salt was dissolved in 180 mL of hot *n*-heptane, and then one mmol of NITiPr was added, and the solution was allowed to cool down to room temperature and stored at -5 °C for 1 week. Orange crystals were collected and analyzed well for M-(hfac)₃(NITiPr)(H₂O). Anal. Calcd for EuC₂₅H₂₄F₁₈N₂O₉: C, 30.32; H, 2.24; N, 2.83. Found: 30.28; H, 2.38; N, 2.71. Calcd for GdC₂₅H₂₄F₁₈N₂O₉: C, 30.15; H, 2.43; N, 2.81. Found: C, 30.08; H, 2.34; N, 2.70.

Crystallographic Data Collection and Structure Refinement. The crystal structure of Eu(hfac)₃(NITiPr)(H₂O) was determined from X-ray diffraction data obtained by using an Enraf Nonius CAD4 four-circle diffractometer equipped with a Mo Kα tube and a graphite monochromator. Crystallographic data are given in Table I while a detailed list of the experimental parameters involved in the data collection are reported in Table SI. Cell parameters were determined from 25 machine-centered reflections. Data collection was performed in the ω–2θ scan mode, measuring the intensity of two test reflections every 5 h. Corrections for Lorentz, polarization, and absorption effects were made. Systematic absences were only compatible with the monoclinic space group $P2_1/a$.

The europium ion was located from the Patterson map. The positional parameters of the other non-hydrogen atoms were defined by successive Fourier and difference Fourier syntheses. The last stage of the refinement procedure, including hydrogen atoms in calculated positions, converged to an R value of 0.0774, and the resulting difference Fourier map showed peaks of no chemical significance. The computer programs used in the crystal structure determination are reported in ref 11.
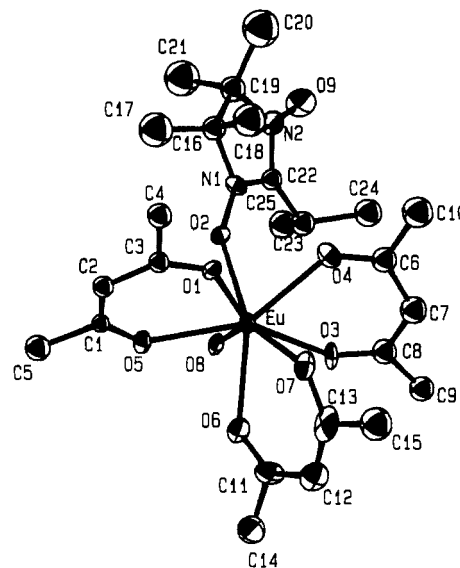
The unit cell parameters of Gd(hfac)₃(NITiPr)(H₂O) were determined from 25 machine-centered reflections.

Physical Measurements. The EPR spectrum was recorded on a Varian E9 spectrometer operating at X-band frequency equipped with an Oxford ESR9 continuous-flow cryostat.
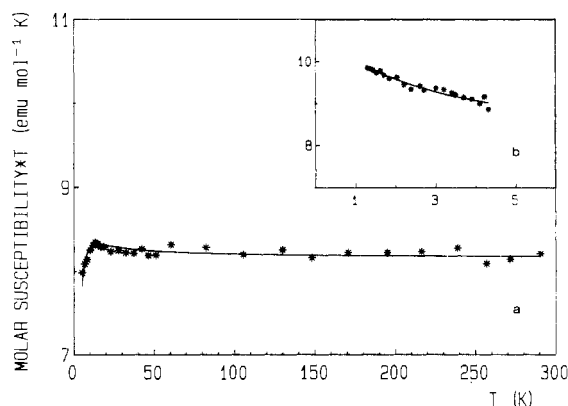
The magnetic susceptibility was measured in the 300–4.2 K temperature range with a DSM5 magnetometer equipped with a Bruker BE-15 electromagnet operating at 1.4 T and an Oxford Instrument CF1200S continuous-flow cryostat and in the 4.2–1.2 K temperature range with an AC mutual-inductance bridge at nearly zero field. The sample was immersed in liquid helium, and the temperature was measured by means of a carbon resistance thermometer calibrated against the vapor pressure of helium.

Results and Discussion

The crystal structure of Eu(hfac)₃(NITiPr)(H₂O) is built up by isolated molecules consisting of a nitronyl nitroxide radical

(1) Bencini, A.; Benelli, C.; Caneschi, A.; Dei, A.; Gatteschi, D. *Inorg. Chem.* **1986**, *25*, 572.
(2) Benelli, C.; Caneschi, A.; Gatteschi, D.; Guillou, O.; Pardi, L. *Inorg. Chem.* **1990**, *29*, 1750.
(3) Benelli, C.; Caneschi, A.; Gatteschi, D.; Pardi, L.; Rey, P.; Shum, D. P.; Carlin, R. L. *Inorg. Chem.* **1989**, *28*, 272.
(4) Benelli, C.; Caneschi, A.; Gatteschi, D.; Pardi, L.; Rey, P. *Inorg. Chem.* **1989**, *28*, 275.
(5) Benelli, C.; Caneschi, A.; Gatteschi, D.; Pardi, L.; Rey, P. *Inorg. Chem.* **1989**, *28*, 3230.
(6) Benelli, C.; Caneschi, A.; Gatteschi, D.; Pardi, L.; Rey, P. *Inorg. Chem.*, in press.
(7) Kahn, O. *Struct. Bonding (Berlin)* **1987**, *68*, 89.
(8) Ullman, E. F.; Osieki, J. H.; Boocock, D. G. B.; Darcy, R. *J. Am. Chem. Soc.* **1972**, *94*, 7049.
(9) Lanchen, M.; Wittag, T. W. *J. Chem. Soc. C* **1966**, 2300.
(10) Richardson, M. F.; Wagner, D. F.; Sands, D. E. *J. Inorg. Nucl. Chem.* **1968**, *30*, 1275.
(11) (a) Sheldrick, G. SHELX-76 System of Computing Programs. University of Cambridge, England, 1976. (b) Rizzoli, C.; Sangermano, V.; Calestani, G.; Andreetti, G. D. CRYSRULER PACKAGE. Università degli Studi di Parma, 1986.

Figure 1. ORTEP drawing of the asymmetric unit of Eu(hfac)₃(NITiPr)(H₂O).

Figure 2. Temperature dependence of the χT product of Gd(hfac)₃-(NITiPr)(H₂O): (a) high-temperature data, the curve representing the best fit obtained for $J = -0.83$ cm⁻¹ and $g = 1.99$. (b) low-temperature data, best fit parameters of $J = -0.65$ cm⁻¹ and $g = 2.00$.

coordinated to Eu(hfac)₃ units, a water molecule completing the coordination sphere of the metal ion. The geometry of the coordination sphere of the europium(III) ion is similar to that observed in other lanthanide–nitronyl nitroxide complexes with the metal ion in a highly distorted dodecahedral environment.[3,5] The ORTEP drawing of the asymmetric unit is reported in Figure 1 while in Table III are reported selected bond distances and angles, positional parameters of the most significant atoms in the structure are given in Table II. The gadolinium derivative, with cell parameters $a = 16.192$ (7) Å, $b = 14.503$ (3) Å, $c = 17.668$ (4) Å, and $\beta = 115.45$ (4)°, is isomorphous with the europium compound, and we assume in the following that the two compounds are also isostructural.

The effective magnetic moment of Gd(hfac)₃(NITiPr)(H₂O) increases on decreasing temperature, in line with a ferromagnetic coupling between the gadolinium(III) and radical spins. The decrease in the χT product below 10 K observed in the set of data measured in a field of 1.4 T is due to saturation effects. In Figure 2, we report the plot of the magnetic data in the form of the χT vs T product. The fit of these data using the isotropic exchange Hamiltonian was performed separately in the high-temperature and low-temperature ranges to account for the different magnetic field strength. The values of the parameters are $J = -0.83$ cm⁻¹ and $g = 1.99$ with $R = 1.00 \times 10^{-3}$ for the 300–4.2 K temperature range and $J = -0.65$ cm⁻¹ and $g = 2.00$ with $R = 1.00 \times 10^{-2}$. The ground state is $S = 4$, and this is confirmed by the EPR spectrum shown in Figure 3 where eight features, corresponding

Figure 3. X-Band powder EPR spectra at liquid-helium temperature for Gd(hfac)$_3$(NITiPr)(H$_2$O).

to the fine structure splitting of the ground state, are clearly resolved.

The experimental magnetic data were fitted also with the dipolar spin Hamiltonian

$$H = DS_{1z}S_{2z}$$

in order to take into account the possibility that anisotropic spin–spin interaction such as dipolar coupling between metal and radical explain the experimental data. Although the agreement with experimental data is not too bad, no quantitative fit could be obtained. The values of D required are, however, larger than 1.0 cm^{-1}. This value is much larger than expected for the dipolar interaction between gadolinium and radical. For this type of system, the point dipolar approximation gives an upper limit to the D value:[5] assuming that the unpaired electron on the radical is localized on the oxygen atom that is bound to gadolinium, the calculated value of D is 0.17 cm^{-1}. This is clearly an overestimation of the dipolar interaction, because the unpaired electron is almost equally shared between the two N–O groups. In a more accurate calculation performed by putting half an electron on the midpoint of each N–O group of the nitronyl nitroxide, we obtained a D value of 0.03 cm^{-1}. Sample calculations on copper–nitronyl nitroxide complexes, performed by using a MO formalism previously described,[5,12,13] provided D values of 0.1 cm^{-1}, and an experimental estimation of the anisotropic exchange in Cu(hfac)$_2$TEMPOL[14] (TEMPOL = 4-hydroxy-2,2,6,6-tetramethylpiperidinyl-N-oxyl) indicated values in the range 0.1–0.2 cm^{-1}. The fact that the EPR spectra of Gd(hfac)$_3$(NITiPr)(H$_2$O) show the presence of a ground $S = 4$ state, with a zero-field splitting of about 600 G, indicates that the dipolar interaction in the lanthanide–radical derivatives must be much smaller than the isotropic one.

The experimental data were fitted also with a complete Hamiltonian including both dipolar and exchange contributions and fixing the g parameter at the value of 2.00: the best fit values are $J = -0.52$ cm^{-1} and $D_{zz} = 0.037$ cm^{-1} with $R = 1.00 \times 10^{-2}$ in the high-temperature range and $J = -0.64$ cm^{-1} and $D_{zz} = 0.041$ cm^{-1} with $R = 1.05 \times 10^{-2}$ for the 4.2–1.2 K temperature range. Therefore, although the dipolar interaction may not be totally negligible, the present data confirm that indeed gadolinium(III) and nitronyl nitroxides are ferromagnetically coupled in an essentially isotropic way.

The present result confirms our previous assumption of ferromagnetic coupling between lanthanide ions and radicals and, adding one more example, lend credibility to our claim of the involvement of the 6s atomic orbitals of the metal ion in the mechanism of exchange. The possibility of a spin-transfer

Table II. Positional Parameters and Isotropic Thermal Factors of Eu(hfac)$_3$(NITiPr)(H$_2$O)^a

	x	y	z	B_{eq}, Å^2
Eu	0.60498 (7)	0.43306 (9)	0.18545 (9)	3.73 (5)
O1	0.550 (1)	0.438 (1)	0.289 (1)	4.1 (7)
O2	0.642 (1)	0.583 (1)	0.229 (1)	4.1 (9)
O3	0.724 (1)	0.376 (1)	0.155 (1)	5.0 (7)
O4	0.743 (1)	0.421 (2)	0.314 (1)	5.6 (3)
O5	0.447 (1)	0.485 (1)	0.121 (1)	4.6 (5)
O6	0.531 (1)	0.336 (1)	0.065 (1)	6.2 (4)
O7	0.616 (1)	0.281 (2)	0.237 (2)	6.3 (1)
O8	0.594 (1)	0.522 (1)	0.063 (1)	4.6 (5)
O9	0.898 (2)	0.765 (2)	0.338 (2)	11 (1)
N1	0.703 (1)	0.639 (1)	0.278 (1)	4.2 (3)
N2	0.821 (1)	0.727 (1)	0.327 (1)	4.1 (4)
C16	0.696 (2)	0.694 (2)	0.344 (2)	6.0 (7)
C17	0.603 (3)	0.712 (4)	0.330 (3)	13 (1)
C18	0.715 (3)	0.615 (3)	0.414 (3)	11 (2)
C19	0.766 (2)	0.757 (3)	0.370 (2)	7.3 (8)
C20	0.830 (4)	0.778 (4)	0.464 (4)	6.7 (7)
C21	0.722 (4)	0.850 (4)	0.326 (4)	7.0 (8)
C22	0.780 (2)	0.657 (2)	0.272 (2)	4.9 (6)
C23	0.815 (2)	0.616 (3)	0.215 (2)	7.0 (8)
C24	0.914 (2)	0.570 (3)	0.266 (2)	9.3 (9)
C25	0.818 (3)	0.688 (3)	0.156 (3)	10 (1)

^{a} Standard deviation in the last significant digits are in parentheses.

Table III. Selected Bond Distances (Å) and Angles (deg) for Eu(hfac)$_3$(NITiPr)(H$_2$O)^a

Distances

Eu–O1	2.36 (1)	Eu–O2	2.31 (1)	Eu–O3	2.36 (1)
Eu–O4	2.40 (2)	Eu–O5	2.42 (1)	Eu–O6	2.40 (2)
Eu–O7	2.36 (2)	Eu–O8	2.46 (2)	O1–C3	1.28 (2)
O3–C8	1.24 (3)	O4–C6	1.23 (3)	O5–C1	1.24 (2)
O6–C11	1.21 (3)	O7–C13	1.31 (5)	O2–N2	1.29 (2)
O9–N2	1.30 (2)				

Angles

O1–Eu–O2	81.4 (5)	O1–Eu–O3	143.7 (6)
O1–Eu–O4	77.0 (5)	O1–Eu–O5	71.4 (5)
O1–Eu–O6	119.3 (5)	O1–Eu–O7	73.7 (7)
O1–Eu–O8	139.5 (5)	O2–Eu–O3	106.7 (6)
O2–Eu–O4	75.7 (6)	O2–Eu–O5	86.1 (6)
O2–Eu–O6	144.2 (6)	O2–Eu–O7	142.3 (7)
O2–Eu–O8	72.4 (6)	O3–Eu–O4	71.3 (5)
O3–Eu–O5	142.9 (6)	O3–Eu–O6	74.6 (6)
O3–Eu–O7	79.8 (6)	O3–Eu–O8	74.8 (5)
O4–Eu–O5	145.5 (5)	O4–Eu–O6	134.4 (6)
O4–Eu–O7	71.4 (7)	O4–Eu–O8	123.4 (5)
O5–Eu–O6	75.2 (5)	O5–Eu–O7	111.3 (6)
O5–Eu–O8	76.4 (5)	O6–Eu–O7	73.4 (8)
O6–Eu–O8	73.7 (6)	O7–Eu–O8	142.7 (7)
Eu–O2–N1	147 (1)	Eu–O1–C3	136 (1)
Eu–O3–C8	135 (2)	Eu–O5–C1	133 (1)
Eu–O4–C6	135 (2)	Eu–O6–C11	134 (2)
Eu–O7–C13	131 (3)		

^{a} Standard deviation in the last significant digits are in parentheses.

mechanism involving these empty orbitals was postulated[15] to explain the origin of the pure Fermi contact contribution in the NMR spectra of lanthanide complexes.

Supplementary Material Available: Full crystallographic details (Table SI), complete positional parameters and isotropic thermal factors (Table SII), anisotropic thermal parameters (Table SIII), and complete bond distances and angles (Table SIV) (8 pages); observed and calculated structure factors (Table SV) (7 pages).

(12) Hefui, M. A.; McConnell, N. M.; Rietmeijer, F. J.; Gribnau, M. C. M.; Keijzers, C. P. *Mol. Phys.* **1986**, *57*, 1283.

(13) Gribnau, M. C. M. Ph.D. Thesis, University of Nijmegen, 1988.

(14) Bencini, A.; Benelli, C.; Gatteschi, D.; Zanchini, C. *J. Am. Chem. Soc.* **1984**, *106*, 5814.

(15) Watson, R. E.; Freeman, A. J. *Phys. Rev.* **1967**, *156*, 251.